*IOSR Journal Of Applied Physics (IOSR-JAP)*
*e-ISSN: 2278-4861.Volume 15, Issue 3 Ser. II (May. – June. 2023), PP 22-28*
*www.Iosrjournals.Org*

# Catalogue Of Potential Magnetic Topological Insulators From Materials Database

Md Rakibul Karim Akanda
*Department of Engineering Technology, Savannah State University—Savannah, GA 31404, United States of America*

***Abstract:***
*Due to the quantum anomalous Hall effect (QAHE), magnetic topological insulators (TI) provide dissipation-free edge transport. However, there are only a small number of magnetic topological insulators that are known. This research identifies a huge number of magnetic topological insulators. Topological insulators with magnetic characteristics are found using data from two materials databases, considering the spin polarization of the unit cell at the Fermi level, magnetization per atom, and magnetization per cell. In addition to classifying, a machine learning model is employed to detect other magnetic topological materials by making use of a large variety of material attributes. The implementation of the quantum anomalous Hall effect (QAHE) at high temperatures will be made possible by a huge number of magnetic TI.*
***Key Word****: Topological Insulator; Magnetic Materials; Machine Learning; Materials Database; Spintronics.*

---

Date of Submission: 01-06-2023 Date of Acceptance: 10-06-2023

---

## I. Introduction

With the various prospective applications like dissipation less edge transport due to quantum anomalous Hall effect (QAHE), topological magneto-electric effect, topological magneto-optical effect, spintronic functionalities having nonlinear unidirectional magnetoresistance and high spin Hall angle, magnetic topological insulators are having growing interest of research community.[1–7] Topological insulators and topological semimetals are becoming new frontiers of research and can offer various functionalities similar to transistors.[8–26] Magnetic materials and magnetic topological insulators are receiving more and more attention in the recent years.[27–32] To achieve QAHE, spontaneous magnetization is needed instead of external magnetic field. For this purpose, magnetic topological insulators (TIs) are generally made by transition metal doping. For example $(Bi,Sb)_2Te_3$ (BST) is doped with Cr, V and Mn. But the Curie temperature of magnetic TIs is a few tens of Kelvins for a moderate doping level. The Curie temperature increases with the doping level, but dopants also create disorder which eventually affects QAHE. An alternative route towards the higher temperature realization of the QAHE is to incorporate the magnetic proximity effect. Generally TI is sandwiched between two ferromagnetic insulators with high Curie temperature (EuS, $Cr_2Ge_2Te_6$, YIGand TIG). Besides this approach of high temperature realization of TIs, the $MB_2T_4$-family materials (M = transition-metal or rare-earth element, B = Bi or Sb, T = Te, Se, or S) have attracted significant attention due to their inherent magnetization ($MnBi_2Te_4$ is an example). The monolayer is predicted to be an magnetic insulator for varying element of M (Ti, V, Mn, Ni,Eu) and their phonon dispersions are found in the literature. Considering their thickness, these materials behave as an axion insulators with Chern number, C = 0 in even number of layers and become quantum anomalous Hall (QAH) insulators with C = 1 in odd number of layers. But still the temperature at which QAHE can be achieved is only up to 4.5 K. Temperature at which QAHE can be achieved needs to be higher to use magnetic topological insulators in industry applications.

This study identifies a significant number of intrinsic magnetic topological insulators, which expands the field of materials research and paves the way for the experimental demonstration of the quantum anomalous Hall effect at higher temperatures. Recent initiatives have been made to leverage materials databases to uncover numerous topological insulators. Using magnetization data from a materials database, magnetic topological insulators are retrieved from these topological insulators. A few additional magnetic topological insulators are found using machine learning approach in addition to these two. Along with their magnetization statistics, certain recently discovered magnetic topological insulators' band structures are provided.

## II. Method

Topological Materials Database [topologicalquantumchemistry.com] provides total 4,321 topological insulator (TI) which were originally found from ICSD materials database. Total 4,321 topological insulators (TI) were found in the Topological Materials Database, which may be accessed at topologicalquantumchemistry.com. The Automatic FLOW (Aflow) [http://aflowlib.org] materials database, which contains 60,325 materials with ICSD tags, is searched for these topological insulators (Fig. 1). 455 topological insulators are discovered to have spin polarization at Fermi level that is larger than zero after paramagnetic or nonmagnetic materials were eliminated from the list of TI materials that were present in the Aflow database.

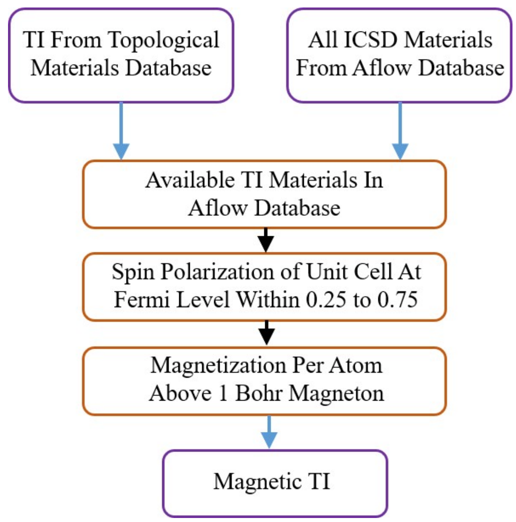


**Figure 1.** flowchart for determining magnetic topological insulators out of materials that are simultaneously listed in both the Topological Materials Database and the Aflow Materials Database and have the ICSD tag.

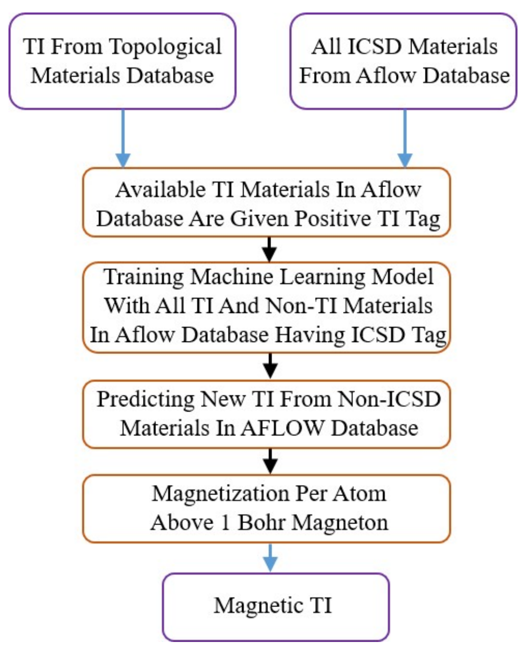


**Figure 2.** Flowchart for applying a machine learning algorithm to distinguish magnetic TI from materials without ICSD tags.

| | Group | Polarization | Moment per Atom($\mu_B$) |
|---|---|---|---|
| MnRh | 221 (Pm-3m) | 0.375308 | 2.54044 |
| $B_2Gd$ | 191 (P6/mmm) | 0.346653 | 2.47534 |
| $CeCo_8Mn_4$ | 139 (I4/mmm) | 0.42245 | 2.43938 |
| $C_3Fe_{17}Ho_2$ | 166 (R-3m) | 0.321525 | 2.35146 |
| $C_3Er_2Fe_{17}$ | 166 (R-3m) | 0.281013 | 2.34616 |
| $Mn_2NdSi_2$ | 139 (I4/mmm) | 0.476767 | 2.19403 |
| $GaFe_2Co$ | 225 (Fm-3m) | 0.451509 | 2.09263 |
| $Mn_2Sb_2Yb$ | 164 (P-3m1) | 0.384063 | 1.99097 |
| $SrMn_2Sb_2$ | 164 (P-3m1) | 0.263674 | 1.98692 |
| $Fe_2Ge_2Nd$ | 139 (I4/mmm) | 0.456738 | 1.98096 |
| $BaMn_2Sb_2$ | 139 (I4/mmm) | 0.275589 | 1.95873 |
| $Fe_2NdSi_2$ | 139 (I4/mmm) | 0.749423 | 1.87554 |
| $Fe_3Se_4$ | 12 (C2/m) | 0.417269 | 1.86067 |
| $Ge_2Mn_2Sr$ | 139 (I4/mmm) | 0.300165 | 1.73069 |
| $Ge_2Mn_2Yb$ | 139 (I4/mmm) | 0.348794 | 1.71251 |
| $DyGe_2Mn_2$ | 139 (I4/mmm) | 0.258104 | 1.62617 |
| $Mn_2Si_2Th$ | 139 (I4/mmm) | 0.317836 | 1.62291 |
| $DyMn_2Si_2$ | 139 (I4/mmm) | 0.342696 | 1.59548 |
| $ErMn_2Si_2$ | 139 (I4/mmm) | 0.300883 | 1.58879 |
| $Cr_4U$ | 87 (I4/m) | 0.392315 | 1.49104 |
| $CeFe_2Ge_2$ | 139 (I4/mmm) | 0.270352 | 1.46693 |
| $CaGe_2Mn_2$ | 139 (I4/mmm) | 0.531608 | 1.44171 |
| AuPr | 221 (Pm-3m) | 0.682797 | 1.43658 |
| $Mn_2S_4Sn$ | 65 (Cmmm) | 0.653758 | 1.42778 |
| $Fe_7Nb_6$ | 166 (R-3m) | 0.647596 | 1.40032 |

**Table 1.** Part-1 of identified magnetic topological insulators which have ICSD tag. The space group, the unit cell's Fermi level spin polarization, and the magnetization per atom are all displayed.

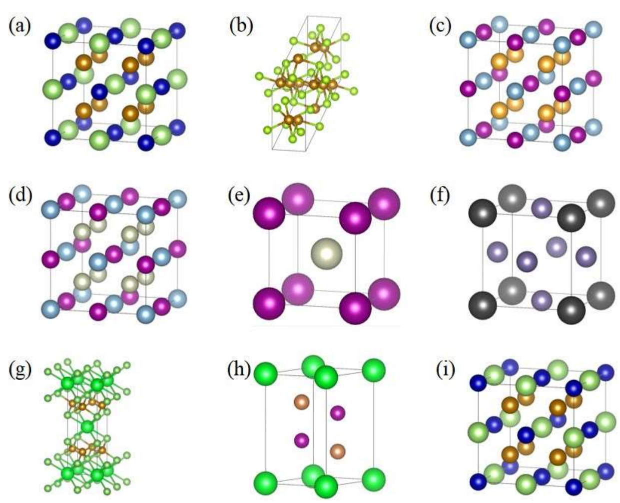


**Figure 3.** Unit cell structure of some identified magnetic topological materials: (a) $CaFe_2As_2$, (b) $Fe_3Se_4$, (c) $MnAlAu_2$, (d)$MnAlRh_2$, (e) MnRh, (f) $PuGe_3$, (g) $SrFe_2As_2$, (h) $SrMn_2Sb_2$, (i) $GaFe_2Co$.

| | Group | Polarization | Moment per Atom($\mu_B$) |
|---|---|---|---|
| $CaFe_2As_2$ | 139 (I4/mmm) | 0.393105 | 1.38434 |
| $CdCu_2Nd_2$ | 65 (Cmmm) | 0.540909 | 1.38215 |
| $Al_8Mn_4U$ | 139 (I4/mmm) | 0.454842 | 1.37541 |
| $B_6Fe_3Pr_4$ | 166 (R-3m) | 0.523744 | 1.35104 |
| AgPr | 221 (Pm-3m) | 0.355468 | 1.34174 |
| $GdMn_2Si_2$ | 139 (I4/mmm) | 0.426179 | 1.33711 |
| $ErFe_6Ga_6$ | 71 (Immm) | 0.290458 | 1.32759 |
| $Fe_2Si_2Yb$ | 139 (I4/mmm) | 0.493325 | 1.24471 |
| $Al_8Cr_4Gd$ | 139 (I4/mmm) | 0.272686 | 1.22723 |
| $MnAlRh_2$ | 225 (Fm-3m) | 0.302948 | 1.22407 |
| $PuGe_3$ | 221 (Pm-3m) | 0.520987 | 1.18466 |
| $Al_8CaMn_4$ | 139 (I4/mmm) | 0.438069 | 1.16135 |
| $Fe_2Si_2Zr$ | 139 (I4/mmm) | 0.314701 | 1.15057 |
| $GdSn_4Ti_6$ | 166 (R-3m) | 0.735934 | 1.14793 |
| $DyFe_2Si_2$ | 139 (I4/mmm) | 0.503306 | 1.14548 |
| $As_2Co_2Nd$ | 139 (I4/mmm) | 0.730453 | 1.14179 |
| $Al_8Mn_4Th$ | 139 (I4/mmm) | 0.362908 | 1.12451 |
| $SrAs_2Fe_2$ | 139 (I4/mmm) | 0.308873 | 1.12139 |
| $MnAlAu_2$ | 225 (Fm-3m) | 0.250696 | 1.11648 |
| $Cu_2InMn$ | 225 (Fm-3m) | 0.254598 | 1.1052 |
| $Mn_2Si_2Yb$ | 139 (I4/mmm) | 0.393555 | 1.08173 |
| $Ga_2Gd$ | 191 (P6/mmm) | 0.392402 | 1.07775 |
| $AlCu_2Mn$ | 225 (Fm-3m) | 0.250066 | 1.06962 |
| $Al_8Fe_4Nd$ | 139 (I4/mmm) | 0.39693 | 1.06959 |
| PrSb | 225 (Fm-3m) | 0.280469 | 1.05381 |

**Table 2.** Part-2 identified magnetic topological insulators which have ICSD tag. Space group, spin polarization of unit cellat Fermi level and magnetization per atom are shown.

| | Group | Moment per Atom($\mu_B$) | Moment per Cell($\mu_B$) |
|---|---|---|---|
| AgAlCr | 216 - F43m | 1.12052 | 3.36155 |
| BiV | 65 - Cmmm | 1.04088 | 2.08177 |
| AgAlMn | 216 - F43m | 1.73379 | 6.93518 |
| $Bi_2V$ | 164 - P3m1 | 1.02988 | 3.08965 |

**Table 3.** Identified magnetic topological insulators using machine learning algorithm from the materials which do not have ICSD tag.

We choose a polarization range of 0.25 to 0.75 to look for prospective magnetic TIs because most common ferromagnetic materials (Fe or Co) have spin polarization at Fermi levels of around 0.5 while ferromagnetic half metals have spin polarization of one (the greatest conceivable value). A total of 50 materials were discovered to be magnetic topological insulators after only those materials are chosen that have magnetism per atom of greater than one Bohr magneton. Using the QUANTUM-ESPRESSO software, first-principle calculations are used to determine the band structure of various magnetic TI materials. The findings section displays the spin polarized band structure together with spin orbit coupling (SOC).

A further machine learning method is then used to find more magnetic Tis (Fig. 2). To do this, the AFLOW materials database's first 21 ICSD material attributes that can be found are extracted. They include topological materials that are mentioned in the Topological Quantum Chemistry database. The machine learning model is trained using these data using the extreme gradient boosting (XGBOOST) technique. A trained model is used to forecast topological insulators from materials in the AFLOW database that are missing the ICSD tag. Utilizing the magnetic moment data of all these projected topological insulators is necessary to identify magnetic topological insulators with magnetization per atom higher than one Bohr magneton.

## III. Results

For 50 identified magnetic topological materials with ICSD tags, space group, spin polarization of the unit cell at Fermi level, and atom-level magnetization are displayed in Tables 1 and 2. Table 3 provides details of detected magnetic topological insulators from non-ICSD materials using machine learning algorithms. In both situations, only topological insulators with magnetic moments per atom greater than one Bohr magneton are taken into consideration.

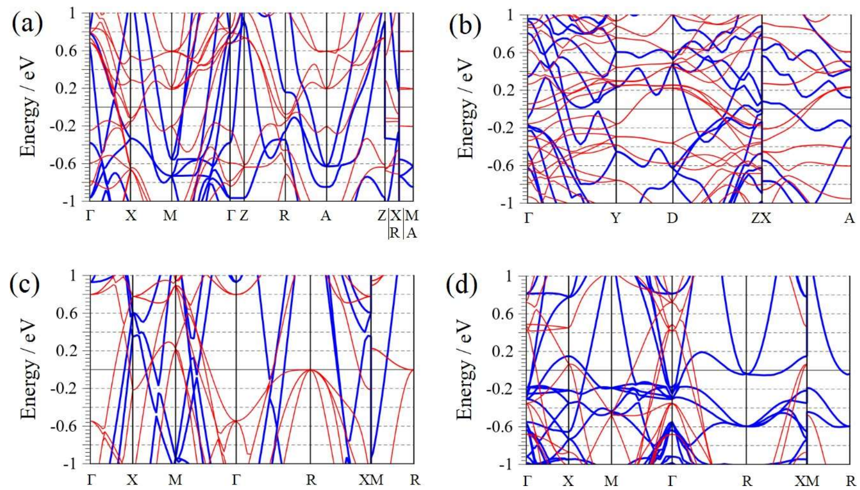


**Figure 4.** Calculated band structure of some identified magnetic topological materials: (a) $CaFe_2As_2$, (b) $Fe_3Se_4$, (c)$MnAlAu_2$, (d) $MnAlRh_2$. Blue color denotes up spin and red color denotes down spin.

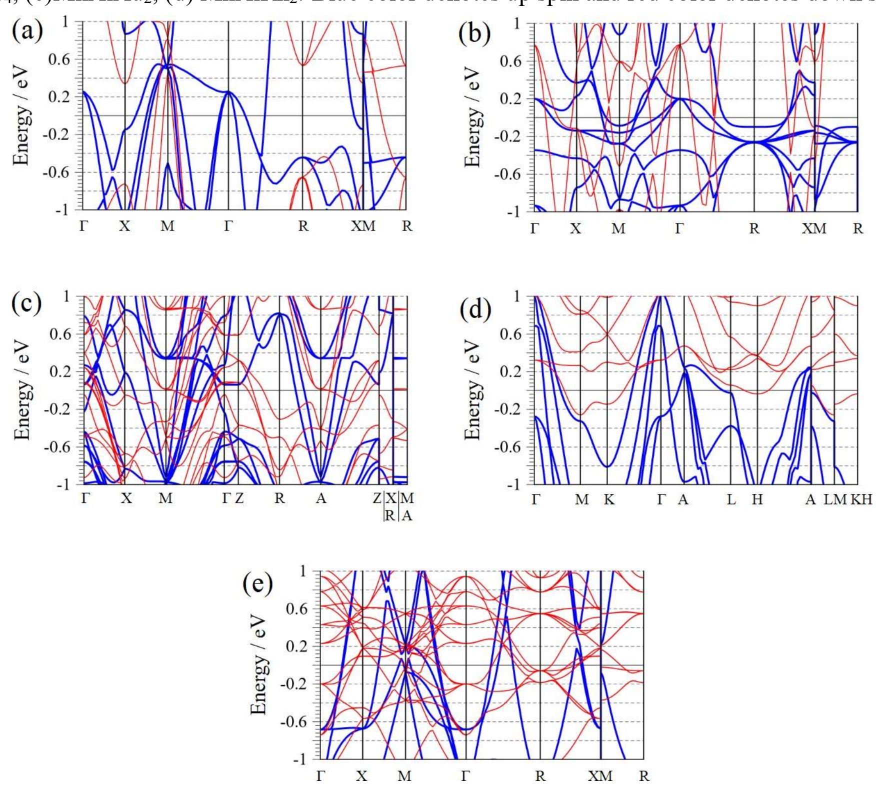


**Figure 5.** Calculated band structure of some identified magnetic topological materials: (a) MnRh, (b) $PuGe_3$, (c) $SrFe_2As_2$, (d) $SrMn_2Sb_2$, (e) $GaFe_2Co$. Blue color denotes up spin and red color denotes down spin.

Some of the magnetic TIs' unit cell structures are depicted in Figure 3 together with their band structures in Figures 4 and 5. $CaFe_2As_2$ has topological indices of $Z_2 = 1$, $Z_4 = 1$, $Z_8 = 5$, and magnetic moment per unit cell of 6.92 Bohr magneton. $Fe_3Se_4$ has topological indices of $Z_4 = 1$, and magnetic moment per unit cell of

13.02 Bohr magneton. $MnAlAu_2$ has topological indices of $Z_2 = 1$, $Z_4 = 1$, $Z_8 = 5$, and magnetic moment per unit cell of 4.47 Bohr magneton. $MnAlRh_2$ has topological indices of $Z_4 = 2$, $Z_8 = 2$, and magnetic moment per unit cell of 4.9 Bohr magneton. MnRh has topological indices of $Z_{4\pi} = 2, Z_8 = 4$, and magnetic moment per unit cell of 5.08 Bohr magneton. $PuGe_3$ has topological indices of $Z_2 = 1$, $Z_{2w,3} = 1$, $Z_4 = 3$, $Z_{4\pi} = 1$, $Z_{2w,1} = 1$, $Z_{2w,2} = 1$, $Z_8 = 7$, and magnetic moment per unit cell of 4.74 Bohr magneton. $SrFe_2As_2$ has topological indices of $Z_2 = 1$, $Z_{2w,3} = 1$, $Z_4 = 3$, $Z_{2w,1} = 1$, $Z_{2w,2} = 1$, $Z_8 = 7$, and magnetic moment per unit cell of 5.6 Bohr magneton. $SrMn_2Sb_2$ has topological indices of $Z_{2w,3} = 1$, $Z_4 = 1$, and magnetic moment per unit cell of 9.93 Bohr magneton. $GaFe_2Co$ has topological indices of $Z_2 = 1$, $Z_4 = 1$, $Z_8 = 5$, and magnetic moment per unit cell of 8.37 Bohr magneton.

As the results are from two materials database and the Topological Materials Database do not have $MnBi_2Te_4$ as a topological insulator, it is not shown in the result. But $MnBi_2Te_4$ is mentioned in the introduction as it has been gaining research interests for the last few years. Some of the identified materials are antiferromagnetic topological insulator e.g., $GdMn_2Si_2$, $ErMn_2Si_2$, $SrAs_2Fe_2$. $GdMn_2Si_2$ can be made as a layered antiferromagnet and can be of future research interest to explore thickness dependent property. Not all materials share the same characteristic. However, when a machine learning model is trained using known topological insulators, unit cell valence electron quantity and number of atoms in unit cell are discovered to be the most prominent features. Two materials databases were used to find the results, one of which solely included topological materials. Once more, several of the predicted materials have previously been demonstrated to be topological insulators, demonstrating the veracity of the findings.

## IV. Conclusions

Using two materials databases, many magnetic topological insulators are found. To distinguish magnetic TI from non-ICSD materials, machine learning is also applied. These many different materials will make it easier for experimenters to investigate QAHE at greater temperatures because of the possibility of dissipation-less edge transport caused by QAHE.

## V. Acknowledgement

This work was supported as part of Modeling and Simulation Program (MSP) grant funded by the US Department of Education under Award No. P116S210002.

## References

[1]. Qi, X. L., Hughes, T. L. & Zhang, S. C. Topological field theory of time-reversal invariant insulators. Phys. Rev. B 78,195424, DOI: 10.1103/PhysRevB.78.195424 (2008).

[2]. Essin, A. M., Moore, J. E. & Vanderbilt, D. Magnetoelectric polarizability and axion electrodynamics in crystallineinsulators. Phys. Rev. Lett. 102, 146805, DOI: 10.1103/PhysRevLett.102.146805 (2009).

[3]. Tokura, Y., Seki, S. & Nagaosa, N. Reports on Prog. Phys. 77, 7, DOI: 10.1088/0034-4885/77/7/076501 (2014).

[4]. Kurumaji, T. *et al.* Optical magnetoelectric resonance in a polar magnet $(Fe, Zn)_2mo_3o_8$ with axion-type coupling. *Phys. Rev. Lett.* **119**, 077206, DOI: 10.1103/PhysRevLett.119.077206 (2017).

[5]. McIver, J. W., Hsieh, D., Steinberg, H., Jarillo Herrero, P. & Gedik, N. *Nat. Nanotechnologys* **7**, 96, DOI: 10.1038/nnano.2011.214 (2012).

[6]. Okada, K. N. *et al.* Enhanced photogalvanic current in topological insulators via fermi energy tuning. *Phys. Rev. B* **93**,081403, DOI: 10.1103/PhysRevB.93.081403 (2016).

[7]. Han, W., Otani, Y. & Maekawa, S. *npj Quantum Mater.* **27**, 3, DOI: 10.1038/s41535-018-0100-9 (2018).

[8]. Aftab, T. & Sabeeh, K. Anisotropic magnetic response of weyl semimetals in a topological insulator multilayer. *J. Appl.Phys.* **127**, 163905, DOI: 10.1063/1.5142216 (2020).

[9]. Wang, Z., Wei, Q., Xu, H.-Y. & Wu, D.-J. A higher-order topological insulator with wide bandgaps in lamb-wave systems.

[10]. *J. Appl. Phys.* **127**, 075105, DOI: 10.1063/1.5140553 (2020).

[11]. Reza, A. K. & Roy, K. Topological semi-metal na3bi as efficient spin injector in current driven magnetic tunnel junction. *J.Appl. Phys.* **126**, 233901, DOI: 10.1063/1.5087077 (2019).

[12]. Lyu, M. *et al.* Large anisotropic magnetocaloric effect in ferromagnetic semimetal pralsi. *J. Appl. Phys.* **127**, 193903, DOI: 10.1063/5.0007217 (2020).

*[13].* Ali, A., Shama & Singh, Y. Rotating magnetocaloric effect in the ferromagnetic weyl semi-metal co3sn2s2. *J. Appl. Phys.* 155107, DOI: 10.1063/1.5120005 (2019).

[14]. Gupta, S., Kanai, S., Matsukura, F. & Ohno, H. Magnetic and transport properties of sb2te3 doped with high concentrationof cr. *Appl. Phys. Express* **10**, 103001, DOI: 10.7567/apex.10.103001 (2017).

[15]. Otrokov, M. M., Chulkov, E. V. & Arnau, A. Breaking time-reversal symmetry at the topological insulator surface bymetal-organic coordination networks. *Phys. Rev. B* **92**, 165309, DOI: 10.1103/PhysRevB.92.165309 (2015).Otrokov, M. M. *et al. JETP Lett.* **105**, 297–302, DOI: 10.1134/S0021364017050113 (2017).

[16]. Otrokov, M. M., Klimovskikh, I. I., Bentmann, H. & et al. *Nature* **576**, 416–422, DOI: 10.1038/s41586-019-1840-9 (2019).

[17]. Otrokov, M. M. *et al.* Unique thickness-dependent properties of the van der waals interlayer antiferromagnet $mnbi_2te_4$ films. *Phys. Rev. Lett.* **122**, 107202, DOI: 10.1103/PhysRevLett.122.107202 (2019).

[18]. Biswas, D. & Maiti, K. Exceptional surface states and topological order in bi2se3. *J. Electron Spectrosc. Relat. Phenom.* **208**, 90 – 94, DOI: https://doi.org/10.1016/j.elspec.2015.11.007 (2016). Special Issue: Electronic structure and function from state-of-the-art spectroscopy and theory.

[19]. Biswas, D., Thakur, S., Balakrishnan, G. & Maiti, K. *Sci. Reports* **5**, 17351, DOI: 10.1038/srep17351 (2015).

[20]. Biswas, D., Thakur, S., Ali, K., Balakrishnan, G. & Maiti, K. *Sci. Reports* **5**, 10260, DOI: 10.1038/srep10260 (2015).

[21]. Adhikary, G. *et al.* Complex temperature evolution of the electronic structure of cafe2as2. *J. Appl. Phys.* **115**, 123901, DOI:

10.1063/1.4869397 (2014).

[22]. Islam, M. S., Akanda, M. R. K., Anwar, S. & Shahriar, A. Analysis of resistances and transconductance of sic mesfet considering fabrication parameters and mobility as a function of temperature. *ICECE 2010* 5–8, DOI: 10.1109/ICELCE.2010.5700539 (2010).

[23]. Akanda, M. R. K., Islam, R. & Khosru, Q. D. M. A physically based compact model for finfets on-resistance incorporating quantum mechanical effects. *ICECE 2010* 203–205, DOI: 10.1109/ICELCE.2010.5700663 (2010).

[24]. Akanda, M. R. K. & Khosru, Q. D. M. Fem model of wraparound cntfet with multi-cnt and its capacitance modeling. *IEEE Transactions on Electron Devices* **60**, 97–102, DOI: 10.1109/TED.2012.2227968 (2013).

[25]. Islam, M. S. & Akanda, M. R. K. 3d temperature distribution of sic mesfet using green's function. *ICECE 2010* 13–16, DOI: 10.1109/ICELCE.2010.5700541 (2010).

[26]. Akanda, M. R. K. & Khosru, Q. D. M. Analysis of output transconductance of finfets incorporating quantum mechanical and temperature effects with 3d temperature distribution. *ISDRS* 1–2, DOI: 10.1109/ISDRS.2011.6135292 (2011).

[27]. Gupta, S., Matsukura, F. & Ohno, H. Properties of sputtered full heusler alloy cr2mnsb and its application in a magnetic tunnel junction. *J. Phys. D: Appl. Phys.* **52**, 495002, DOI: 10.1088/1361-6463/ab3fc6 (2019).

[28]. Gupta, S., Kanai, S., Matsukura, F. & Ohno, H. Ferromagnetic resonance spectra of py deposited on (bi1-xsbx)2te3. *AIP Adv.* **7**, 055919, DOI: 10.1063/1.4974891 (2017).

[29]. Akanda, M. R. K. & Lake, R. K. Magnetic properties of NbSi2N4, VSi2N4, and VSi2P4 monolayers. *Appl. Phys. Lett.* **119**, 052402 DOI: 10.1063/5.0055878 (2021).

[30]. Akanda, M. R. K. Park, I. J. & Lake, R. K. Interfacial dzyaloshinskii moriya interaction of antiferromagnetic materials. *Phys. Rev. B* **102**, 224414, DOI: 10.1103/PhysRevB.102.224414 (2020).

[31]. Akanda, M. R. K. Catalog of magnetic topological semimetals. *AIP Advances* **10**, 095222, DOI: 10.1063/5.0020096 (2020).

[32]. Akanda, M. R. K. Scaling of voltage controlled magnetic anisotropy based skyrmion memory and its neuromorphic application. *Nano Ex.* **3**, 025003, DOI: 10.1088/2632-959X/ac6bb5 (2022).